Title

Magnesian calcite solid solution thermodynamics inferred from authigenic deep-sea carbonate

Authors

Lammers, Laura Nielsen
Mitnick, Elizabeth H

Publication Date

2019-03-01

DOI

10.1016/j.gca.2019.01.006

Peer reviewed

Magnesian calcite solid solution thermodynamics inferred from authigenic deep-sea carbonate

Laura Nielsen Lammers[a,b]* & Elizabeth H. Mitnick[c]

[a] Department of Environmental Science, Policy and Management, University of California, Berkeley, 130 Mulford Hall, Berkeley, California, 94720, United States.

[b] Energy Geosciences Division, E.O. Lawrence Berkeley National Laboratory, Berkeley, California 94720, United States.

[c] Department of Earth and Planetary Science University of California, Berkeley, California 94720, United States.

*corresponding author, lnlammers@berkeley.edu

ABSTRACT

Magnesian calcite is perhaps the most well studied solid solution in the geosciences due to the widespread use of marine carbonates to reconstruct paleoenvironment. Despite decades of research, the low temperature thermodynamic properties of magnesian calcite in seawater are poorly constrained, largely because very slow reaction kinetics prevent the direct measurement of equilibrium distribution coefficients (K_d^{Mg}) for anhydrous Mg-bearing minerals. In this study, we use the Mg content of authigenic calcite formed in deep-sea marine carbonate sediments to determine the dependence of K_d^{Mg} on temperature and aqueous Mg/Ca between ~2 and 25°C. We find that the solid activity coefficient of magnesite in Mg-calcite is strongly temperature dependent in this range, leading to predicted exsolution of Mg at low temperatures. At the temperatures typical of ocean bottom water, equilibrium Mg distribution coefficients are at least an order of magnitude lower than values inferred from inorganic calcite

growth experiments. Moreover, the equilibrium temperature dependence of K_d^{Mg} agrees well with field-based paleotemperature calibrations determined for low-Mg benthic and planktonic foraminifera at temperatures < 20°C. Partitioning of Mg in foraminiferal tests is expected to be highly dependent on the Mg/Ca ratio in the calcifying fluid, so ignoring secular variations in seawater Mg/Ca can lead to significant underestimation of paleotemperatures.

1. INTRODUCTION

Deep-sea carbonate sediments and their corresponding pore waters host a vast trove of information on ancient seawater chemistry and climate. Carbonate minerals preserve, with varying degrees of fidelity, the isotopic and trace element composition of numerous paleoproxy systems (*i.e.,* $\delta^{18}O$, $\delta^{13}C$, $^{87/86}Sr$, Mg/Ca) that can be used to reconstruct past Earth surface conditions (Shackleton, 1987; Ingram and Sloan, 1992; Elderfield and Ganssen, 2000; Lear et al., 2002) and provide critical insights into climate system responses to perturbations in the global carbon cycle (Schrag et al., 2013). The marine carbonate record primarily consists of aragonite and more thermodynamically stable calcite, which both contain variable amounts of Mg. The extent of Mg substitution in marine biogenic calcite has been shown to be strongly temperature dependent and is the basis for the empirically calibrated Mg/Ca paleotemperature proxy (Elderfield and Ganssen, 2000; Lear et al., 2002). Mg substitution in the calcite lattice controls mineral preservation (Al-Aasm and Veizer, 1982; Brown and Elderfield, 1996; Lea et al., 2000; Fehrenbacher and Martin, 2014; Branson et al.,

2015), but significant uncertainty over the solid solution properties of Mg-calcite means there is no consensus on whether high- or low-Mg marine calcite is more likely to be preserved.

Magnesium partitioning behavior determined from magnesian calcite synthesis (Katz, 1973; Berner, 1975; Mucci and Morse, 1983) and solubility (Chave et al., 1962; Mucci and Morse, 1984; Walter, 1984; Busenberg and Plummer, 1989) experiments have frequently been assumed to reflect equilibrium partitioning behavior (Lea et al., 1999; Kozdon et al., 2013; Branson et al., 2015), although several studies have underscored the influence of kinetics (*e.g.*, (Berner, 1975; De Choudens-Sánchez and González, 2009). These experiments typically give Mg distribution coefficients (K_d^{Mg})—the concentration ratio of Mg/Ca in the solid normalized by that of the fluid—in the range of $K_d^{Mg} \approx 0.01\text{-}0.05$ at 25°C. In contrast, studies of marine carbonate diagenesis suggest that low-Mg calcite persists at the expense of higher Mg calcite in core-top foraminifer tests (Hover et al., 2001), and that recrystallized calcite has a very low Mg content corresponding to $K_d^{Mg} < 0.001$ (Baker et al., 1982; Higgins and Schrag, 2012; Kozdon et al., 2013; Branson et al., 2015). This large discrepancy in K_d^{Mg} has been explained in terms of a reaction with a separate, lower Mg/Ca fluid in the marine carbonate sediment during diagenesis that is isolated from the bulk pore fluid, although this explanation conflicts with measured Sr distribution data (Kozdon et al., 2013; Branson et al., 2015).

The critical factor limiting our ability to experimentally constrain the magnesian calcite solid solution at temperatures relevant to seawater paleotemperature reconstructions (~0-30°C) is the very slow rate of reaction required to obtain an equilibrium Mg distribution coefficient (Bénézeth et al., 2011). Moreover, the very small excess enthalpies of mixing associated with low-Mg calcite cannot be precisely quantified using calorimetry (Navrotsky and Capobianco, 1987). Recently, an experimental study (Mavromatis et al., 2013) demonstrated that calcite growth rates on order $10^{-8.5}$ mol/m^2/s are required to obtain equilibrium K_d^{Mg} values at 25°C and 1 bar, which is at least 2.5 orders of magnitude slower than the rates of Mg calcite growth in synthesis experiments from which equilibrium Mg partitioning behavior has previously been inferred (Katz, 1973; Mucci and Morse, 1983). The strong rate dependence of Mg partitioning suggests that laboratory studies likely do not reflect true equilibrium K_d^{Mg} values. Slow growth rates are difficult to maintain in a controlled laboratory setting for sufficiently long to obtain precise measurements of trace element composition, and the problem may be compounded at lower temperatures.

Marine calcite sediments experience slow and sustained recrystallization (Richter and DePaolo, 1987; Richter and Liang, 1993; Fantle and DePaolo, 2007) and therefore present an ideal system to constrain equilibrium distribution coefficients for magnesian calcite in

seawater. Reconstructions of Ca and Sr isotope profiles in marine carbonate sediments recovered from the Ontong Java Plateau (OJP) have been used to show that detrital biogenic calcite recrystallizes at saturation states very near equilibrium with respect to pure calcite (Fantle and DePaolo, 2007). We use spatially resolved electron microprobe analysis of these sediments (~ 30 Myr old ODP site 807A) from 710 and 739 meters below the sea floor (mbsf; Figure 1a-c) to determine the Mg contents of biogenic (BC) and authigenic calcite (AC). At these core depths, it is possible to visually distinguish faceted authigenic calcite crystals from the detrital and partially recrystallized biogenic calcite via scanning electron microprobe (SEM) imaging (Fabricius and Borre, 2007). We use these data as well as prior measurements of the Mg content of calcite precipitated at various bottom water temperatures to determine the temperature dependence of the Mg distribution coefficient. A thermodynamic model is developed for the dependence of K_d^{Mg} on both temperature and aqueous Mg/Ca and compared to the Mg/Ca paleotemperature proxy in foraminiferal calcite.

2. METHODS

2.1 Electron microprobe analysis

We analyzed the Mg/Ca ratio of bulk carbonate sediment from Ocean Drilling Program (ODP) Site 807 from samples 75X-2X and 78X-

2W, at depths of 710 and 739 meters below seafloor (mbsf), respectively. Samples were not sorted, powdered, or processed in any way prior to mounting. Sediments were mounted in 1-inch rounds and impregnated with Epo-Tek 301-2 epoxy under vacuum, following the sample preparation procedure reported in Fabricius and Borre (2007). After setting, samples were polished and coated with 25 nm of carbon. Measurements were made on a Cameca SX-100 electron microprobe at the University of California Davis. Maps were collected over two sessions (referred to as Sessions 1 and 2). Element maps were collected under a beam voltage of 15 kV and a raster length of 0.5 µm/ pixel with 500 ms dwell time. Point measurements and standards were collected with 1 µm beam diameter with 15 kV beam voltage.

Mg/Ca molar ratios of point measurements (~5 µm) as a function of instrument count ratios (cts Mg/cts Ca) were calibrated with a 3-point standard curve ($R^2 = 0.99997$) using pure calcite (0 mmol Mg/mol Ca), Icelandic spar (4.6 mmol Mg/mol Ca), and experimentally grown Mg-calcite (29.3 mmol Mg/mol Ca). Although the curve was linear (with $R^2 = 0.99995$) to a much higher molar ratio of 1003.5 mmol Mg/mol Ca (dolomite), this point was excluded to achieve the best possible fit at the lower molar ratios expected in our samples. We accounted for differences between mapped pixel intensities and point measurement intensities by scaling the mean of the pixel ratios taken within 5 µm diameter areas (N = 27899) to the corresponding calibrated

foraminiferal ratios from point measurements, as determined by the aforementioned calibration curve. This scaling factor was then applied to the pixel intensities of authigenic particles. Uncertainties from the calibration curve, 2 standard deviation of the mean (s.d.m.) of point measurements, and 2 s.d.m. of pixel intensities were propagated and are reported in Figure 1. Overall, this approach allowed us to calculate uncertainty in pixel mapping due to counting statistics that are not otherwise captured in point measurement intensities and uncertainty on the calibration curve alone.

We selected areas to map that included cross sections of detrital/ biogenic calcite (*i.e.*, foraminifer tests) as well as visibly faceted or euhedral calcite (Figure 1a-b; Supplementary Information, Figure S1). Carbonate composition was verified with spot analyses. The distinction between biogenic and authigenic carbonate types was initially based on morphology and subsequently confirmed based on distinguishing features in Mg/Ca ratio maps. Point measurements (N = 24) were collected on foraminifer tests, yielding a mean Mg/Ca ratio of 2.78 ± 0.37 (2 s.e.) mmol Mg/mol Ca. Background intensities of Ca and Mg element maps were determined offline during post-processing, after which maps were thresholded to eliminate pixels equal to or less than maximum background counts.

In addition to a clear visual distinction biogenic and authigenic calcite based on crystal morphology observed previously

(Fehrenbacher and Martin, 2014), it is apparent that authigenic crystals and clusters are characterized by higher Mg/Ca rinds surrounding a lower Mg/Ca interior (Figure 1). We obtained pixel transects from the edge of authigenic calcite particles inward (8 transects per particle, 53 particles), capturing the evolution of Mg/Ca ratios from the interior to the exterior high Mg/Ca perimeter of the particle. Transects extend radially from the particle center, and were taken 45° apart to ensure that a random sample was obtained.

2.2 Calculation of equilibrium distribution coefficients from electron microprobe results

The electron microprobe results described above provide the ratio of (x_{mag}/x_{cal}), the ratio of mole fractions of magnesite and calcite in the authigenic Mg calcite. To calculate equilibrium K_d^{Mg} from these measured Mg contents, we assume that the Mg composition of the authigenic particle exteriors reflect equilibration with the pore fluid with which it is currently in contact: c_{Ca} = 20.7 mM, c_{Mg} = 38.3 mM, c_{Mg}/c_{Ca} = 1.85, T = 10.3 ± 0.1°C, and P = 363 bars, based on pore fluid data from Kroenke et al. (Kroenke et al., 1991) and on down-hole temperature and pressure data for ODP site 807A available for download online: http://brg.ldeo.columbia.edu/data/odp/leg130/807A/. In addition, we assume that the authigenic calcite precipitated unidirectionally from the interior outwards, with the homogeneous particle interiors (> 3 µm from the edge; Figure 1) representing early

crystallization at the core-top. We estimate the fraction of the total authigenic carbonate deposited as a function of time using the recrystallization rate-age relationships derived from Sr concentrations and Ca isotopes (Fantle and DePaolo, 2007), which show that the rate of total carbonate recrystallization decays exponentially with sediment age. Assuming that recrystallization is unidirectional, the majority of authigenic calcite would have been formed during early recrystallization, with 60% of the material formed within the first 5 million years post-deposition. The interior of the AC sampled in Figure 1 of the main text was likely formed at the end of the Paleogene, when the seawater Mg/Ca was approximately 40% of modern (Lowenstein et al., 2001; Horita et al., 2002; Coggon et al., 2010; Gothmann et al., 2015), and bottom water temperatures were likely slightly greater than today (~4°C) (Zachos et al., 1994; Hansen et al., 2013). For the interior authigenic calcite, we therefore assume c_{Mg}/c_{Ca} = 2 ± 1, T = 4 ± 2 °C, and P = 285 bars, which provides us with an additional, lower-T constraint on the equilibrium K_d^{Mg} (Table 1).

3. THERMODYNAMIC MODELING

The equilibrium partitioning behavior of calcite ($CaCO_3$) and magnesite ($MgCO_3$) in solid solution can be described in terms of measurable quantities by the distribution coefficient,

$$K_d^{Mg} = \left(\frac{x_{mag}}{x_{cal}} \right) \Big/ \left(\frac{c_{Mg}}{c_{Ca}} \right) \quad [1]$$

where x_{mag} and x_{cal} are the mole fractions of magnesite (mag) and calcite (cal) in the solid solution ($x_{mag} + x_{cal} \approx 1$), and c_i is the total aqueous concentration of *i*. Distribution coefficients are related to solid activity coefficients through the expressions for the end-member ion activity products:

$$a_{Ca^{2+}} a_{CO_3^{2-}} = K_{sp,cal} x_{cal} \gamma_{cal}$$

$$a_{Mg^{2+}} a_{CO_3^{2-}} = K_{sp,mag} x_{mag} \gamma_{mag}, \quad [2]$$

where $K_{sp,i}$ represents the solubility product of either calcite or magnesite, and γ represents the corresponding solid activity coefficients in the solid solution at the pressure and temperature of interest. Unit activity of the solid solution is assumed to represent the pure phase. Total ion activity coefficients $\gamma_{T,i}$ can be used to correct the free aqueous ion activity to the total (free and complexed) concentration (Mucci, 1983), for example,

$$a_{Mg^{2+}} = \gamma_{T,Mg^{2+}} c_{Mg}. \quad [3]$$

Combining Eqs. 1-3, the equilibrium K_d^{Mg} at a given T and P is given by,

$$K_d^{Mg} = \frac{K_{sp,cal} \gamma_{cal} \gamma_{T,Mg^{2+}}}{K_{sp,mag} \gamma_{mag} \gamma_{T,Ca^{2+}}}. \quad [4]$$

We model the temperature and pressure dependence of Mg partitioning in calcite using Eq. 4. The values of end-member solubilities and total aqueous ion activity coefficients can be calculated based on previous work as described below, leaving the solid end-member activity coefficients as unknowns that are determined here, based on equilibrium K_d^{Mg} values in the temperature range 2-25°C (Table 1). The following sub-sections detail the methods used to calculate each variable in Eq. 4 to obtain K_d^{Mg} as a function of T and P.

3.1 End-member solubilities as a function of temperature

Calcite solubility ($K_{sp,cal}$) is determined as a function of temperature (in degrees Kelvin) using the expression (Plummer and Busenberg, 1982),

$$\log_{10} K_{sp,cal} = -171.9065 - 0.077993T + 2839.3/T + 71.595\log_{10} T, \quad [5]$$

and magnesite solubility is calculated using an expression that is consistent with the revised Helgeson-Kirkham-Flowers equation of state (Bénézeth et al., 2011),

$$\log_{10} K_{sp,mag} = 7.267 - 0.033918T - 1476.604/T. \quad [6]$$

3.1.1 Pressure correction to end-member solubility products

For each solid solution end-member, K_{sp} was first calculated at the relevant temperature at atmospheric pressure, and then corrected

for higher pressures using formulations and coefficients that account for both molar volume and compressibility effects (Millero, 1982),

$$\ln\left(\frac{K_{sp,P}}{K_{sp,1\,bar}}\right) = \frac{-\Delta V P}{RT} + \frac{\Delta K P^2}{2RT}, \qquad [7]$$

where temperature T is in Kelvin, R is the gas constant. The partial molar volume (ΔV) and compressibility (ΔK) changes of the reaction at atmospheric pressure are given,

$$\Delta V = \sum_i \bar{V}_{i,\text{products}} - \sum_i \bar{V}_{i,\text{reactants}}$$

$$\Delta K = \sum_i \bar{K}_{i,\text{products}} - \sum_i \bar{K}_{i,\text{reactants}}, \qquad [8]$$

and the partial molar volumes ($\bar{V}$) and compressibilities ($\bar{K}$) of the products and reactants were determined with the following formulations, with temperature t in °C:

$$\bar{V}(T) = \bar{V}(0^\circ C) + A_v t + B_v t^2$$

$$\bar{K}(T) = \bar{K}(0^\circ C) + A_k t. \qquad [9]$$

3.2 Calculation of total aqueous ion activity coefficients

Two different models for seawater speciation, an ion association approach and a Pitzer approach, were used in PHREEQC to determine the ratio of total ion activity coefficients ($\gamma_{T,Mg^{2+}} / \gamma_{T,Ca^{2+}}$) for Eq. 4 at different temperatures and pressures. A narrow range of values was

obtained, from 1.15 for modern seafloor water recorded at ODP site 807 (2°C, 285 bars) down to 1.10 at standard temperature and pressure (25°C, 1 bar). This difference (less than 5%) in the total activity ratio yields errors on the theoretical K_d^{Mg} that are much less than the errors due to variability in the measured Mg content of authigenic calcite, so we consider the pressure and temperature effects to be negligible. A total ion activity coefficient ratio $\gamma_{T,Mg^{2+}} / \gamma_{T,Ca^{2+}} = 1.15$ is assumed for the model fitting described below.

3.3 Thermodynamic model for solid activity coefficients γ_{cal} and γ_{mag}

End-member solid activity coefficients γ_{cal} and γ_{mag} are required to calculate the theoretical K_d^{Mg} expression given in Eq. 4. Modeling the complete solid solution behavior for magnesian calcite requires a constraint of the partitioning behavior of Ca in magnesite and dolomite across the miscibility gap (Nordstrom and Munoz, 1986). In the absence of these data, we treat the low-Mg solid solution using a subregular model for binary solutions, which captures the observed dependence of K_d^{Mg} on both temperature and aqueous Mg/Ca. According to this model, the solid end-member activity coefficients are given by

$$RT \ln \gamma_{cal} = x_{mag}^2 \left[W_{12} + 2(W_{21} - W_{12})(1 - x_{mag}) \right], \text{ and} \qquad [10]$$

$$RT\ln\gamma_{mag} = (1 - x_{mag})^2 \left[W_{21} + 2(W_{12} - W_{21}) x_{mag} \right], \quad [11]$$

where W_{21} and W_{12} are empirical interaction parameters in units of kJ/mol. At the limit of small x_{mag}, the value of γ_{cal} converges to 1, and γ_{mag} converges to the regular solution model, which depends on a single interaction paramter, W_{21}. While a regular solution model can be used to accurately capture $K_d^{Mg}(T)$, this model predicts an increase in K_d^{Mg} with an increase in fluid Mg/Ca (Supplementary Information, Figure S2). Several inorganic calcite growth studies as well as foraminiferal culturing studies have shown that Mg partitioning behavior follows the opposite trend (Mucci and Morse, 1983; Evans and Müller, 2012). Accounting for subregular solution behavior allows us to simultaneously model the effects of temperature, fluid Mg/Ca, and growth kinetics on Mg partitioning.

The end-member activity coefficient model (*e.g.* Eqs. 10-11) was fitted in two stages. First, we calculate the T dependence of the W_{21} interaction parameter assuming that this value reflects regular solution behavior. Such an assumption is expected to be valid at the very low $MgCO_3$ contents of the measured calcite given in Table 1. Substituting Eqs. 10 and 11 and our value of the total ion activity coefficient ratio into Eq. 4 and solving for W_{21} at the limit of small x_{mag}, we obtain

$$W_{21}(T) \approx RT\ln\left(\frac{K_d^{Mg}}{1.15} \cdot \frac{K_{sp,mag}(T)}{K_{sp,cal}(T)} \right). \quad [12]$$

The maximum value of x_{mag} in the calcite data used for these calculations is 0.006, which introduces an error in W_{21} that is much less than the error due to uncertainties in K_d^{Mg} and in temperature. Second, we estimate a fixed value of the W_{12} interaction parameter based on the aqueous Mg/Ca dependence of inorganic calcite precipitation experiments (Mucci and Morse, 1983). Because the Mg/Ca dependence of K_d^{Mg} is only known for fast inorganic growth experiments and foraminiferal culturing experiments at ambient temperatures, we do not attempt to fit a T-dependent value of W_{12}. Thus, the model will not necessarily predict any temperature variability in the K_d^{Mg} dependence on aqueous Mg/Ca with accuracy. Moreover, the experiments used to fit W_{12} were conducted at high growth rates relative to the equilibrium Mg partitioning limit of $\sim 10^{-8.5}$ mol/m^2/s (Mavromatis et al., 2013), so a reasonable value for this parameter is estimated using a full kinetic model for Mg uptake during growth (Nielsen et al., 2013), substituting the end-member activity coefficients given in Eqs. 10 and 11 (see Supplementary Information for more details). According to this kinetic model, the dominant effect of fast growth is to shift the K_d^{Mg} at a given fluid Mg/Ca to higher values. Given the lack of near-equilibrium data for Mg partitioning over a wide range of Mg/Ca, the value of the W_{12} parameter is subject to a large degree of uncertainty, and improving this estimate should be the subject of future work. Finally, we assume that both the W_{21} and W_{12} interaction parameters are independent of

pressure, which is reasonable for the low and similar-compressibility solid end-members, and we attribute all of the temperature dependence of the solid solution not captured by solid end-member solubilities to a temperature-dependent W_{21} interaction parameter.

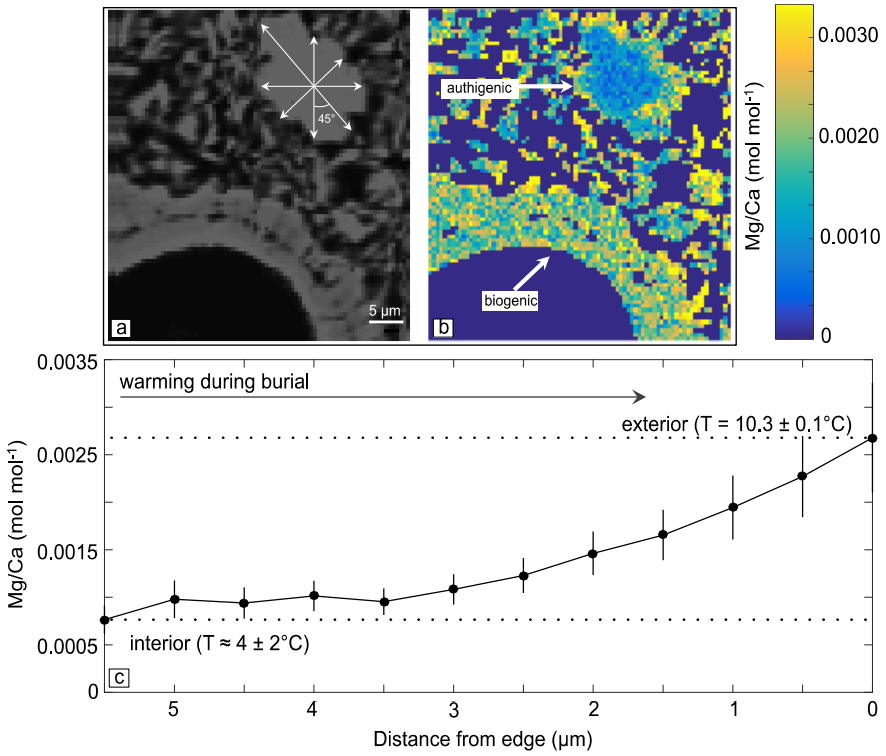

Figure 1. Spatial distribution of Mg in authigenic and biogenic calcite from ODP site 807 marine carbonate sediment. Electron microprobe (a) BSE maps and (b) corresponding Mg/Ca ratios show euhedral authigenic calcite crystals adjacent to foraminiferal shell fragments. (c) Average Mg/Ca ratios for the AC (± 2 s.e., N=53) obtained by averaging transects (8 per particle) through each particle as illustrated in (a) increase systematically from the particle center to the edge, indicating enhanced Mg uptake due to sediment warming during burial diagenesis.

4. RESULTS

The results of our elemental analyses give an average Mg content of the biogenic calcite in shell fragments (x^{BC}_{MgCO3} = 0.0028 ± 0.0004, 2 s.e., N fragments = 24) significantly higher than that of the average bulk abiogenic calcite ($x^{AC,bulk}_{MgCO3}$ = 0.0021 ± 0.0003, 2 s.e., N particles = 53; $p < 0.001$), with all values at least an order of magnitude lower than the range of values expected based on distribution coefficients obtained from experiments conducted in either seawater or simple electrolyte solutions (cf. Busenberg and Plummer, 1989). Interestingly, the Mg content of the authigenic calcite decreases systematically from the particles' exteriors inwards, reflecting a trend towards greater Mg uptake during burial diagenesis (Figure 1c). The significant variability in Mg content around the exterior of these particles is characteristic of recrystallized calcite and may reflect asymmetric growth of vicinal faces on calcite crystals leading to variable trace element incorporation (Paquette and Reeder, 1995).

Using measured pore fluid Mg and Ca contents and calculated values for Mg and Ca total ion activity coefficients (see Methods), we calculate the distribution coefficient of abiogenically precipitated calcite in equilibrium with modern pore fluid to be K_d^{Mg} = 0.0014 ± 0.0001 at 10.3 ± 0.1°C and 363 ± 5 bars. This value is close to the value assumed by Higgins & Schrag (2012) to reconstruct the ODP carbonate pore fluid Mg and Ca profiles. The Mg content of the interior of the authigenic calcite crystals gives K_d^{Mg} = 0.0005 ± 0.0002

corresponding to a pore fluid Mg/Ca ratio of ~2 ± 1 and a bottom water temperature of 4 ± 2°C (see Methods), which agrees with the value obtained by Branson et al. (2015) for core-top recrystallized calcite in modern seawater (Table 1).

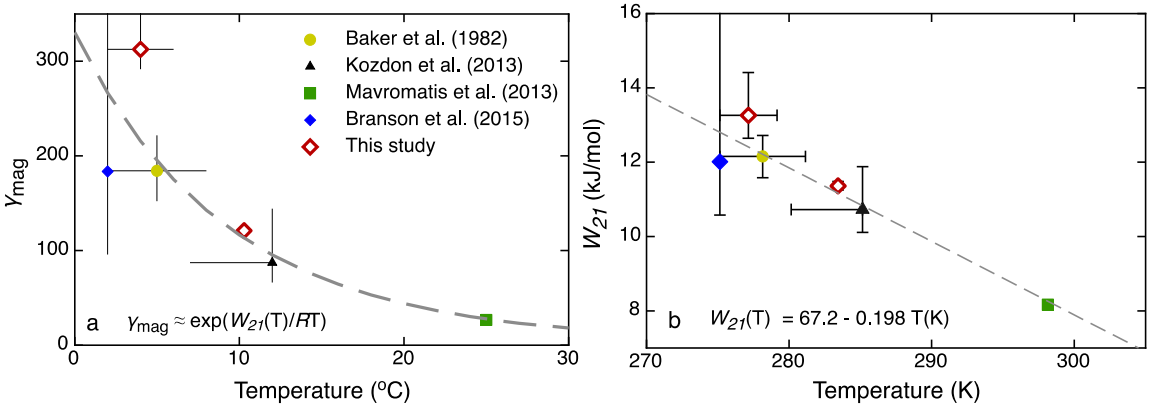

Figure 2. (a) Solid activity coefficients for magnesite in Mg calcite as a function of temperature. The strong temperature dependence of the solid activity coefficient indicates highly non-ideal solid solution behavior. (b) Calculated interaction parameter (W_{21}; Eq. 10) used to model $MgCO_3$ solid solution in calcite. A large positive value of W_{21} is consistent with excess enthalpies of mixing expected for disordered Mg calcite and dolomite (Navrotsky and Capobianco, 1987; Burton and Van de Walle, 2003). The linear dependence on temperature at low-T should not be extrapolated to higher temperatures.

Table 1. Summary of measured Mg partitioning data assumed to reflect equilibrium values. Pressures for core top data are determined based on hydrostatic seawater pressure at depth. Uncertainties included in the tabulated data are accounted for in the linear fit to the interaction parameter $W_{21}(T)$. Uncertainties on measured values are given as 1 standard deviation unless otherwise noted, and asymmetric uncertainties are given in square brackets.

Temp. (°C)	P (bars)	(c_{Mg}/c_{Ca})	x_{mag} (×10³)	K_d^{Mg}	W_{21} (kJ/mol)	Note (Ref.)
			Literature values			
2±0.7[a]	281	5.2	3.7±3.3[c]	0.0075±0.007	12.0 [10.6,17.0]	Branson et al. (2015)
5±3[b]	286	4.64±0.5	3.75	0.0008±0.0001	12.2 [11.6,12.7]	Baker et al. (1982)

≤12	153	3.1±1	6.2	0.0020±0.0007	10.7 [10.1,11.9]	Kozdon et al. (2013)
25	1	0.06-0.66	1.6[d]	0.0082±0.0003	8.2 [8.1,8.3]	Mavromatis et al. (2013)
10.3±0.1	363	1.85±0.1	2.7±0.6	0.0014±0.0001	11.4 [11.2,11.5]	*This study* *Exterior*
4±2	285	2±1	0.9±0.1	0.0005±0.0002	13.3 [12.5,14.5]	*Interior*

[a]Bottom water temperatures in the 2-4 km depth range on the Ontong Java Plateau were obtained from Herguera et al. (1992) *Paleoceanography, 7*(3), 273-288.
[b] Temperature uncertainty is approximated.
[c] Uncertainty is given as the intra-quartile range (IQR).
[d] Calculated from distribution coefficient assuming an intermediate aqueous $(c_{Mg}/c_{Ca})_{fl}$ = 0.2. Resulting interaction parameter uncertainty estimates are calculated assuming fluid elemental ratios on the high and low ends of the $(c_{Mg}/c_{Ca})_{fl}$ range provided.

4.1 Temperature dependence of Mg partitioning in calcite

We use our measured equilibrium K_d^{Mg} values, along with literature values obtained from recrystallized abiogenic calcite (Katz, 1973; Kozdon et al., 2013; Branson et al., 2015) and from calcite growth experiments extrapolated to near-equilibrium (Mavromatis et al., 2013), to fit a subregular solution thermodynamic model for the T-dependent solid activity coefficients for magnesite in magnesian calcite (Bénézeth et al., 2011) down to 2°C (Figure 2a). A plot of the calculated W_{21} interaction parameter values as a function of T is given in Figure 2b for the K_d^{Mg} values listed in Table 1, which we assume to represent equilibrium Mg partitioning behavior in seawater. Uncertainties on W_{21} were calculated as the minimum and maximum values determined based on the composite errors on individual measurements in the calculation, including K_d^{Mg}, $x_{mag,}$ and temperature.

Fitting was performed using the polynomial algorithm in the modeling software ProFit. The fitted interaction parameter decreases linearly with temperature between 2 and 25°C according to

$$W_{21} = 67.2(8.9) - 0.198(0.032) \times T(^{\circ}K) \quad [13]$$

Removing the interior calcite analyzed in this study from the regression yields a slope and intercept that are within the 1σ confidence intervals for the coefficients given, so this model is insensitive to the pore fluid conditions assumed in our calculation of interior K_d^{Mg}. Extrapolation to higher temperatures will likely result in error, so we only consider this model expression to be valid between ~2 and 25°C. Based on Mg distribution coefficients obtained during aragonite recrystallization at elevated temperatures under far from equilibrium growth conditions (Katz, 1973), it appears that the W_{21} interaction parameter may converge to a constant value with increasing temperature. Future work is required to determine equilibrium Mg partitioning behavior in calcite at these higher temperatures.

4.2 Dependence of Mg partitioning in calcite on aqueous Mg/Ca

Seawater Mg/Ca ratios have varied considerably through geologic time (Lowenstein et al., 2001; Coggon et al., 2010; Gothmann et al., 2015), therefore in order to have a robust paleotemperature proxy it is necessary to constrain the influence of aqueous Mg/Ca on the Mg distribution coefficient (Evans and Müller, 2012). Modeled Mg

distribution coefficients assuming a fitted value of the W_{12} interaction parameter of ~40 for fast (non-equilibrium) growth is plotted in Figure 3a, and corresponding equilibrium Mg distribution coefficients are plotted as a function of aqueous Mg/Ca concentration ratio, temperature, and pressure in Figure 3b. We completed a sensitivity analysis to evaluate the impact of the W_{12} parameter on the Mg distribution coefficient for variable aqueous Mg/Ca. For low values of $0 < W_{12} < 17$, the model predicts an increase in K_d^{Mg} with fluid Mg/Ca, similar to a simple regular solution model (see Supplementary Information, Figure S2). A value of this parameter greater than ~17 causes the slope of the K_d^{Mg} vs. Mg/Ca curve to reverse. Based on the results of both inorganic calcite growth experiments (Mucci and Morse, 1983) and of several foraminiferal calcite culturing experiments (Evans and Müller, 2012; Evans et al., 2015), K_d^{Mg} is expected to decrease significantly with increasing fluid Mg/Ca ratio. Fast growth offsets the modeled K_d^{Mg} towards higher values relative to equilibrium but causes relatively minor shifts to the slope of the K_d^{Mg} vs. Mg/Ca fluid curves, so it is unlikely that a kinetic effect alone can cause a reversal in the dependence of Mg distribution coefficient on fluid Mg/Ca ratios. The modeled dependence of solid Mg/Ca concentration ratios on both temperature and fluid Mg/Ca concentrations ratios is plotted in Figure 4.

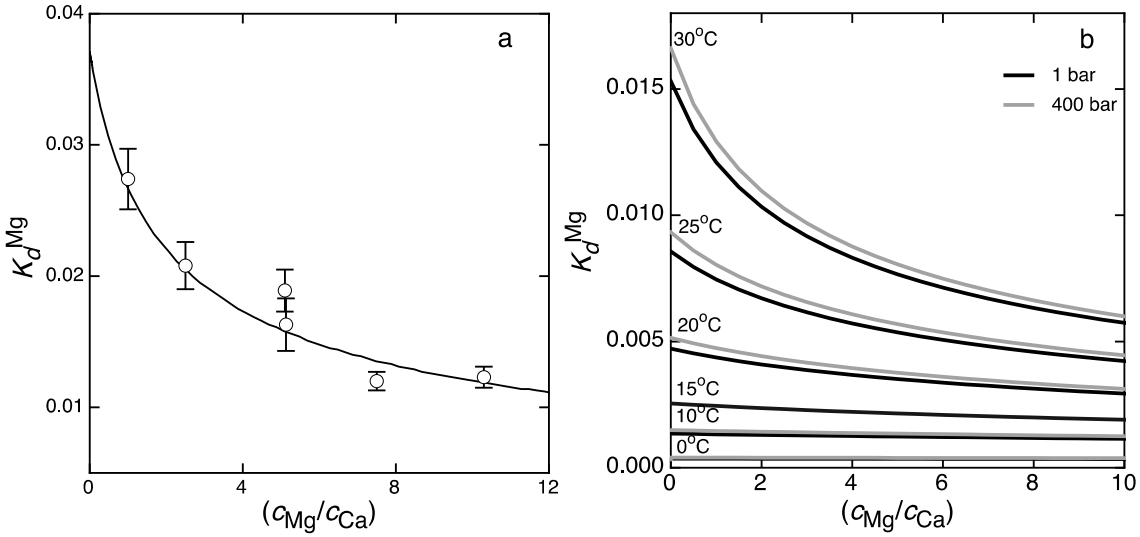

Figure 3. Mg distribution coefficient in calcite as a function of aqueous Mg/Ca. (a) Measured data for non-equilibrium inorganic calcite precipitation from seawater (Mucci and Morse, 1983) used to fit the W_{12} interaction parameter and the corresponding kinetic model curve. (b) Modeled distribution coefficients for calcite precipitated near equilibrium. The vertical scale is larger in (a), because faster growth rates in the inorganic experiments increase the Mg distribution coefficient at a given temperature.

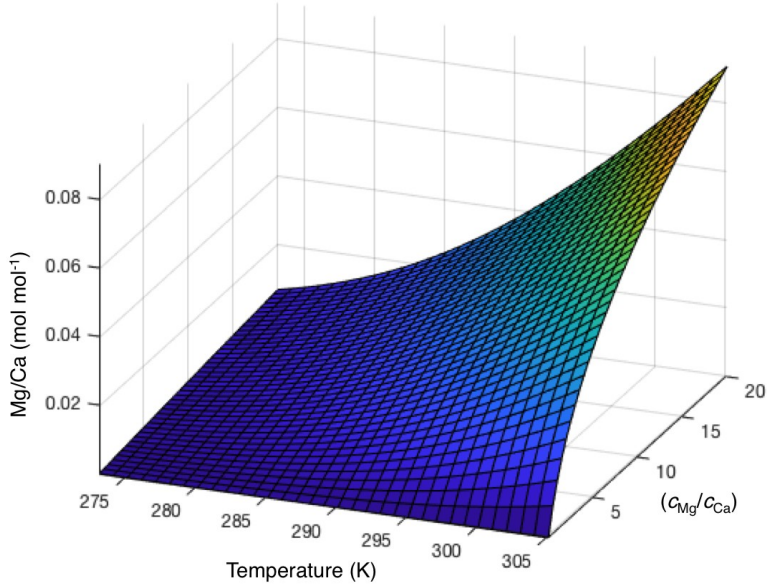

Figure 4. Modeled equilibrium solid calcite Mg/Ca ratio as a function of temperature and fluid Mg/Ca ratio at 1 bar pressure.

5. DISCUSSION

Results of our thermodynamic calculations indicate that the magnesite end-member activity coefficient (Figure 2a) and consequently K_d^{Mg} (Figures 3-4) are strongly dependent on temperature and Mg/Ca in solution but only weakly dependent on pressure. Previous studies of Mg in calcite have assumed constant solid activity coefficients on the basis of magnesian calcite decomposition experiments performed in the range of 600-800°C (Gordon and Greenwood, 1970). In contrast, we find that the activity coefficient for magnesite in low-Mg calcite varies dramatically at low temperature, indicating highly non-ideal solid solution behavior. The strong non-ideality of the low temperature solid solution causes Mg incorporation in excess of a few tenths of a mole percent to destabilize calcite in seawater, possibly acting as a driving force for the sustained recrystallization of detrital calcite. This process results in Mg loss from biogenic calcite during early diagenesis (Land, 1967; Hover et al., 2001), conflicting with studies that concluded high magnesium calcite (> 5-7 mol% Mg) is most thermodynamically stable in seawater (Chave et al., 1962; Winland, 1969; Katz, 1973; Plummer and Mackenzie, 1974).

The large positive value of the solid solution W_{21} interaction parameter extrapolated to low temperature shown in Figure 2b is in qualitative agreement with theoretical results obtained from ground state free energies of mixing for disordered magnesian calcite (Burton

and Van de Walle, 2003). The strong increase in the magnesite activity coefficient with decreasing temperature is also consistent with the activity-composition relations derived from simulations (Vinograd et al., 2006), albeit stronger and shifted towards much lower temperatures. A significant decrease in the interaction parameter with temperature may reflect a tendency towards ordering during calcite precipitation at higher temperatures, as the excess enthalpy of mixing is strongly positive for disordered Mg calcite and negative for ordered Mg calcite (Navrotsky and Capobianco, 1987; Reeder, 2000; Burton and Van de Walle, 2003). Large variations in excess enthalpy of mixing observed over relatively narrow compositional ranges in the Ca-rich dolomites have been attributed to Ca-Mg-ordering (Reeder, 2000), but it is currently not possible to detect Mg ordering in low-Mg calcite.

Given the complexity of seawater and the marine sediment pore fluids, it is possible that coupled substitutions of impurities such as Na^{+}, Sr^{2+} and SO_4^{2-} can impact the Mg calcite solid solution behavior, especially as $MgCO_3$ makes up a diminishing proportion of the solid solution at low temperature. Such higher-order solid solution effects are not discernable with the present data set, but future efforts should be devoted to understanding the surprisingly strong temperature dependence of excess free energies of mixing in low-Mg calcite.

5.1 Magnesian calcite thermodynamics and the foraminiferal Mg/Ca paleotemperature proxy

Foraminiferal calcification is the dominant contributor to the modern marine calcification budget (Schiebel, 2002), and much work has been done to establish accurate foraminiferal calcite Mg/Ca paleotemperature proxies. Numerous field and laboratory based studies have investigated the temperature sensitivity of Mg uptake into foraminiferal tests (typically reported in units of % $°C^{-1}$), which is calculated from the exponential constant determined by exponential regression of solid Mg/Ca vs. temperature data (Nürnberg et al., 1996; Rosenthal et al., 1997; Elderfield and Ganssen, 2000; Lear et al., 2000; Lear et al., 2002; Anand et al., 2003). In addition to temperature, seawater salinity, carbonate chemistry, and pH have long been known to affect foraminiferal Mg/Ca (Nürnberg et al., 1996; Lea et al., 1999; Gray et al., 2018). The temperature sensitivity also varies with species (Nürnberg et al., 1996; Rosenthal et al., 1997), where in general, benthic foraminifera have both higher Mg contents and stronger sensitivities than planktonic species.

Applying our new thermodynamic model, we find that the temperature-dependence of foraminiferal calcite Mg/Ca can be explained by an equilibrium partitioning effect between ~2-20°C. This conclusion is illustrated in Figure 5, which shows the solid calcite Mg/Ca molar ratio calculated assuming best-fit ratios of Mg/Ca in the calcifying fluid, $(c_{Mg}/c_{Ca})_{cfl}$, superimposed on temperature-dependent Mg/Ca molar ratios from an aggregation of field-based (Rosenthal et

al., 1997; Elderfield and Ganssen, 2000; Lear et al., 2002; Gray et al., 2018) and cultured (Nürnberg et al., 1996) foraminiferal calcite data. These theoretical curves capture the strength of the temperature dependence of solid Mg/Ca at low temperatures as well as the increase in slope with increasing Mg content.

When compared with a series of multi-species paleoproxy calibrations (Elderfield and Ganssen, 2000; Lear et al., 2002; Anand et al., 2003), this thermodynamic model agrees well with reported foraminiferal calcite Mg/Ca temperature sensitivities (Supporting Information, Figure S3). However, the model is not a simple exponential function, so no single sensitivity value can be assigned over the entire temperature range. Instead, the model predicts a decrease in temperature sensitivity with increasing temperature. This behavior is in qualitative agreement with foraminiferal calcite data, which suggest a similar trend (Supporting Information, Figure S3). When benthic foraminifera living at < 5°C are excluded from the calibration of Lear et al. (2002) (Lear et al., 2002), the overall temperature sensitivity decreases from 10.9 ± 0.7 to 9.7 ± 1.3% $°C^{-1}$. It is important to note, however, that the temperature sensitivity reported in this study (Lear et al., 2010) may have been affected by diagenetic alteration. For the planktonic species considered here, exponential regression of all field-based Mg/Ca data gives an overall temperature sensitivity of 6.6% $°C^{-1}$ in the range of 0-30°C. This result

is within error of the seawater salinity- and pH- corrected value of 6.0 ± 0.8% $°C^{-1}$ obtained by Gray et al. (2018) for *G. ruber* (white) living at tropical sea-surface temperatures (SST). Regression of the aggregated data from planktonic foraminifera living at a lower range of temperatures (< 20°C), however, yields a significantly stronger temperature sensitivity of 8.7% $°C^{-1}$. Despite this qualitative agreement, at temperatures representative of the tropical sea-surface (> 20°C), the thermodynamic model overestimates the temperature sensitivity of Mg/Ca compared to paleoproxy calibrations (Supporting Information, Figure S3). The model's overestimation of the temperature sensitivity of solid Mg/Ca for tropical SST is consistent with our hypothesis that the W_{21} interaction parameter may converge to a constant value at higher temperatures.

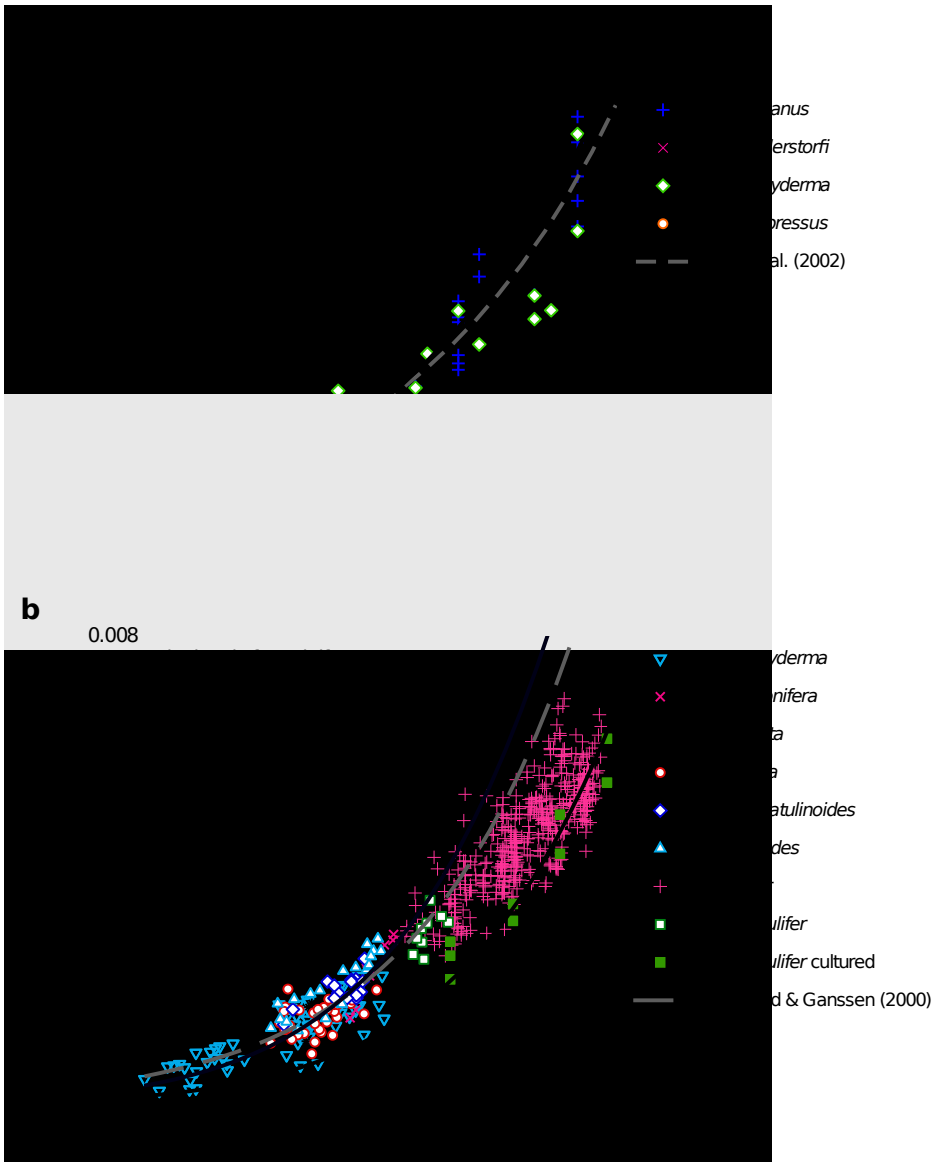

Figure 5. Theoretical temperature dependence of the Mg/Ca ratio in calcite superimposed on (a) benthic and (b) planktonic foraminiferal paleoproxy calibrations. Model curves (solid black) are calculated assuming Mg/Ca ratios in the calcifying fluid labeled on the panels, and shaded regions indicate the range of uncertainties on the W_{21} interaction parameter (Eq. 13). Compared with the field-based Mg/Ca paleotemperature calibration curves (gray dashed), model curves closely capture the temperature dependence, as well as the increase in temperature dependence for higher $(c_{Mg}/c_{Ca})_{cfl}$.

The excellent agreement between the theoretical equilibrium and organism-based temperature calibration curves (Elderfield and

Ganssen, 2000; Lear et al., 2002) is surprising given the prevalence of vital effects in organisms that are typically inferred to have kinetic or biological origins (Lea et al., 1999; Erez, 2003). Estimates of surface area normalized precipitation rates available for planktonic foraminifera range between $10^{-7.95}$ and $10^{-5.95}$ mol/m^2/s and are an order of magnitude lower for benthic species (Carpenter and Lohmann, 1992; Lea et al., 1995; Erez, 2003). Excepting some benthic species, these rates are likely far too rapid to obtain equilibrium Mg partitioning in calcite (Mavromatis et al., 2013).

Far-from-equilibrium growth conditions and subsequent precipitation of high-Mg calcite do not appear to alter the temperature dependence of Mg/Ca or K_d^{Mg} compared with the modeled equilibrium slopes. The strength of the temperature dependence of Mg/Ca modeled here is similar to that of high-Mg calcite synthesized in seawater solutions at higher supersaturations (Mucci, 1987; Oomori et al., 1987; Rosenthal et al., 1997) and also to that of high-Mg foraminiferal calcite (Toyofuku et al., 2000), given precipitation from seawater-like solutions where $(c_{Mg}/c_{Ca})_{cfl} \approx 5.2$. Although the dependencies in the literature are generally reported in units of percent per °C, a meaningful comparison among studies must be done considering the sensitivities in absolute Mg/Ca per °C. Comparing the calculated slope of Mg/Ca vs. temperature in the 5-25°C range with inorganic calcite data from Mucci (1987), we find very similar average

values of 0.0012 °C^{-1} and 0.0013 °C^{-1}, respectively, corresponding to average sensitivities of 10.2% °C^{-1} and 1.7% °C^{-1}. While the magnitude of these slopes in units of Mg/Ca per °C are smaller than those determined at ~10-25°C for inorganic calcite (0.0025°C^{-1} corresponding to 3.2% °C^{-1}; Oomori et al., 1987) as well as cultured high-Mg foraminifera (0.0022 °C^{-1} or 1.8% °C^{-1} for *P. opercularis* and 0.0029 °C^{-1} or 2.5% °C^{-1} for *Q. yabei*; (Toyofuku et al., 2000)), the slope of the model curve at 25°C has a comparable value of 0.0022 °C^{-1} (7.6% °C^{-1}). The present data set cannot explain the underlying cause of the similar temperature dependencies of Mg uptake, especially given the variation in growth environments and formation mechanisms. However, the data demonstrate that the equilibrium temperature dependence of K_d^{Mg} in calcite may be obtained even when the absolute Mg content is much higher than for solids precipitated near equilibrium.

The low $(c_{Mg}/c_{Ca})_{cfl}$ values required to superimpose the model paleoproxy curves on the measured data (*e.g.* ~2.0 for benthic foraminifera, and to ~1.0 and ~0.5 for wild and cultured planktonic foraminifera compared to 5.2 for modern seawater (Broecker and Peng, 1982)) are most easily explained by Mg exclusion from the calcifying fluid. However, they may also be caused by a different vital effect that reduces Mg uptake during calcification. It is unlikely that growth kinetics in the absence of biological effects can account for the

observed shift towards *lower* solid Mg/Ca, because inorganic calcite experiments, which are generally performed at rates exceeding 10^{-8} mol/m^2/s (e.g., Katz, 1973; Mucci and Morse, 1983) have K_d^{Mg} values > 0.01 at 25 °C. It is most likely that the low Mg content in foraminiferal calcite compared to expected values in seawater can be explained by the hypothesis that marine biomineralizing organisms engineer the composition of the calcifying fluid by selectively removing Mg to minimize growth rate inhibition (Bentov and Erez, 2006; Khalifa et al., 2016). The lower fitted $(c_{Mg}/c_{Ca})_{cfl}$ required to model the cultured *G. sacculifer* data in Figure 5b may reflect the fact that significant metabolic energy is expended to remove Mg from the site of calcification by mineralization or ATP buffering (Bentov and Erez, 2006), and may be more readily available to an organism grown in culture than to those in nature. For benthic foraminiferal species that calcify high-Mg calcite tests, including *O. ammonoides*, *O. complanata* (Evans et al., 2013), *H. depressa* (Raitzsch et al., 2010), and *P. opercularis* (Toyofuku et al., 2000), prior researchers have concluded that biocalcification likely occurs from a calcifying fluid with major and trace element chemistry that resembles seawater (Raitzsch et al., 2010; Evans et al., 2015).

The strong dependence of K_d^{Mg} on the fluid Mg/Ca ratio predicted by the model implies that secular changes to Mg/Ca in seawater will significantly impact the Mg content of marine calcite precipitated near

equilibrium, with higher Mg/Ca leading to lower values of K_d^{Mg} (Figure 2). The Mg/Ca ratio in seawater has varied over time, increasing from an Mg/Ca ratio of about 2 around 100 Ma to the modern value of 5.2 (Lowenstein et al., 2001; Horita et al., 2002; Tyrrell and Zeebe, 2004). Several studies have investigated the influence of seawater Mg/Ca on the Mg content and distribution coefficient in foraminiferal calcite (Delaney et al., 1985; Segev and Erez, 2006; Raitzsch et al., 2010; Evans and Müller, 2012; Evans et al., 2015) as well as calcite precipitated far from equilibrium in the laboratory (Mucci and Morse, 1983). In all cases, K_d^{Mg} decreases with increasing seawater Mg/Ca. While the current model has been fitted to reproduce these observations (Figure 3a), more work is necessary to more tightly constrain this dependence at thermodynamic equilibrium.

6. CONCLUSION

Here we used marine authigenic calcite formed during ultra-slow recrystallization to constrain the equilibrium partitioning behavior of Mg in calcite at low temperatures. Data obtained from calibrated electron microprobe maps give average Mg contents of the biogenic calcite in shell fragments that are significantly higher than the average bulk abiogenic calcite. We calculate the distribution coefficient in equilibrium with modern pore fluid to be K_d^{Mg} = 0.0014 ± 0.0001 at 10.3 ± 0.1°C and 363 ± 5 bars, which is at least an order of magnitude

lower than the range of values expected based on distribution coefficients obtained from inorganic calcite growth experiments. We used these values along with several measurements of the Mg content of authigenic calcite precipitated near equilibrium with respect to calcite (Baker et al., 1982; Kozdon et al., 2013; Mavromatis et al., 2013; Branson et al., 2015) to develop a thermodynamic model for the magnesian calcite solid solution. We selected the simplest model capable of reproducing the observed dependence of Mg partitioning on both temperature and fluid Mg/Ca, a subregular solid solution model. The large values of the calculated solid $MgCO_3$ end-member activity coefficients and their strong temperature dependence at low temperature indicate highly non-ideal solid solution behavior. Comparison of our thermodynamic model to multiple Mg/Ca paleoproxy curves based on benthic and planktonic foraminiferal calcite gives surprisingly good agreement, leading us to conclude that these foraminiferal species likely preserve to some extent a thermodynamic partitioning effect.

The difficulty of interpreting the thermodynamic behavior of solid solutions is not unique to magnesian calcite, although it is compounded in this case by the strong influence of Mg-Ca ordering on phase stability (Navrotsky and Capobianco, 1987; Burton and Van de Walle, 2003). Due to the chemical complexity of natural waters, all minerals precipitated in nature will incorporate trace substituents and

other types of defects to some extent during growth. These substituents alter both the bulk thermodynamic properties of the crystals as well as their precipitation, dissolution, and nucleation kinetics, as surface growth mechanisms depend upon the strength of ion binding at the mineral-aqueous interface. The fact that some elements such as Sr obtain phase equilibrium at much faster growth rates than others is likely a reflection of the rate-limiting step of ion desolvation during growth, although the presence of other species such as sulfate have also been implicated (Baker and Kastner, 1981). Future work should focus on elucidating the interdependencies of various ions involved in solid solution formation and the kinetics of mineral growth, with the ultimate aim of being able to simultaneously predict mineral phase stability, surface reaction kinetics and composition in complex natural fluids.

ACKNOWLEDGEMENTS. The authors gratefully acknowledge support from the Director, Office of Science, Office of Basic Energy Sciences, of the U.S. Department of Energy under Contract No. DE-AC02-05CH11231. We also thank our mentor, professor D. DePaolo, for suggesting marine carbonates sediments as a natural laboratory for studying near-equilibirum processes and for his helpful feedback.

REFERENCES

Al-Aasm, I.S. and Veizer, J. (1982) Chemical stabilization of low-Mg calcite: an example of brachiopods. Journal of Sedimentary Research 52, 1101-1109.

Anand, P., Elderfield, H. and Conte, M.H. (2003) Calibration of Mg/Ca thermometry in planktonic foraminifera from a sediment trap time series. Paleoceanography 18, 1050.

Baker, P.A. and Kastner, M. (1981) Constraints on the formation of sedimentary dolomite. Science 213, 214-216.

Baker, P.A., Gieskes, J.M. and Elderfield, H. (1982) Diagenesis of Carbonates in Deep-Sea Sediments--Evidence From SR/CA Ratios and Interstitial Dissolved SR2+ Data. Journal of Sedimentary Research 52, 71-82.

Bénézeth, P., Saldi, G.D., Dandurand, J.-L. and Schott, J. (2011) Experimental determination of the solubility product of magnesite at 50 to 200 C. Chemical Geology 286, 21-31.

Bentov, S. and Erez, J. (2006) Impact of biomineralization processes on the Mg content of foraminiferal shells: A biological perspective. Geochemistry, Geophysics, Geosystems 7.

Berner, R.A. (1975) The role of magnesium in the crystal growth of calcite and aragonite from sea water. Geochimica et Cosmochimica Acta 39, 489-504.

Branson, O., Read, E., Redfern, S.A., Rau, C. and Elderfield, H. (2015) Revisiting diagenesis on the Ontong Java Plateau: Evidence for

authigenic crust precipitation in Globorotalia tumida. Paleoceanography 30, 1490-1502.

Broecker, W.S. and Peng, T.-H. (1982) Tracers in the Sea.

Brown, S.J. and Elderfield, H. (1996) Variations in Mg/Ca and Sr/Ca ratios of planktonic foraminifera caused by postdepositional dissolution: Evidence of shallow Mg-dependent dissolution. Paleoceanography 11, 543-551.

Burton, B.P. and Van de Walle, A. (2003) First-principles-based calculations of the CaCO 3–MgCO 3 and CdCO 3–MgCO 3 subsolidus phase diagrams. Physics and Chemistry of Minerals 30, 88-97.

Busenberg, E. and Plummer, L.N. (1989) Thermodynamics of magnesian calcite solid-solutions at 25 C and 1 atm total pressure. Geochimica et Cosmochimica Acta 53, 1189-1208.

Carpenter, S.J. and Lohmann, K.C. (1992) SrMg ratios of modern marine calcite: Empirical indicators of ocean chemistry and precipitation rate. Geochimica et Cosmochimica Acta 56, 1837-1849.

Chave, K., Deffeyes, K., Weyl, P., Garrels, R. and Thompson, M. (1962) Observations on the solubility of skeletal carbonates in aqueous solutions. Science 137, 33-34.

Coggon, R.M., Teagle, D.A.H., Smith-Duque, C.E., Alt, J.C. and Cooper, M.J. (2010) Reconstructing Past Seawater Mg/Ca and Sr/Ca from

Mid-Ocean Ridge Flank Calcium Carbonate Veins. Science 327, 1114-1117.

De Choudens-Sánchez, V. and González, L.A. (2009) Calcite and Aragonite Precipitation Under Controlled Instantaneous Supersaturation: Elucidating the Role of CaCO3 Saturation State and Mg/Ca Ratio on Calcium Carbonate Polymorphism. Journal of Sedimentary Research 79, 363-376.

Delaney, M.L., Bé, A.W. and Boyle, E.A. (1985) Li, Sr, Mg, and Na in foraminiferal calcite shells from laboratory culture, sediment traps, and sediment cores. Geochimica et Cosmochimica Acta 49, 1327-1341.

Elderfield, H. and Ganssen, G. (2000) Past temperature and δ18O of surface ocean waters inferred from foraminiferal Mg/Ca ratios. Nature 405, 442-445.

Erez, J. (2003) The source of ions for biomineralization in foraminifera and their implications for paleoceanographic proxies. Reviews in Mineralogy and Geochemistry 54, 115-149.

Evans, D. and Müller, W. (2012) Deep time foraminifera Mg/Ca paleothermometry: Nonlinear correction for secular change in seawater Mg/Ca. Paleoceanography and Paleoclimatology 27.

Evans, D., Müller, W., Oron, S. and Renema, W. (2013) Eocene seasonality and seawater alkaline earth reconstruction using

shallow-dwelling large benthic foraminifera. Earth and Planetary Science Letters 381, 104-115.

Evans, D., Erez, J., Oron, S. and Müller, W. (2015) Mg/Ca-temperature and seawater-test chemistry relationships in the shallow-dwelling large benthic foraminifera Operculina ammonoides. Geochimica et Cosmochimica Acta 148, 325-342.

Fabricius, I.L. and Borre, M.K. (2007) Stylolites, porosity, depositional texture, and silicates in chalk facies sediments. Ontong Java Plateau – Gorm and Tyra fields, North Sea. Sedimentology 54, 183-205.

Fantle, M.S. and DePaolo, D.J. (2007) Ca isotopes in carbonate sediment and pore fluid from ODP Site 807A: the Ca 2+(aq)–calcite equilibrium fractionation factor and calcite recrystallization rates in Pleistocene sediments. Geochimica et Cosmochimica Acta 71, 2524-2546.

Fehrenbacher, J.S. and Martin, P.A. (2014) Exploring the dissolution effect on the intrashell Mg/Ca variability of the planktic foraminifer Globigerinoides ruber. Paleoceanography 29, 854-868.

Gordon, T. and Greenwood, H. (1970) The reaction dolomite+ quartz+ water= talc+ calcite+ carbon dioxide. American Journal of Science 268, 225-242.

Gothmann, A.M., Stolarski, J., Adkins, J.F., Schoene, B., Dennis, K.J., Schrag, D.P., Mazur, M. and Bender, M.L. (2015) Fossil corals as an archive of secular variations in seawater chemistry since the Mesozoic. Geochimica et Cosmochimica Acta 160, 188-208.

Gray, W.R., Weldeab, S., Lea, D.W., Rosenthal, Y., Gruber, N., Donner, B. and Fischer, G. (2018) The effects of temperature, salinity, and the carbonate system on Mg/Ca in Globigerinoides ruber (white): A global sediment trap calibration. Earth and Planetary Science Letters 482, 607-620.

Hansen, J., Sato, M., Russell, G. and Kharecha, P. (2013) Climate sensitivity, sea level and atmospheric carbon dioxide. Phil. Trans. R. Soc. A 371, 20120294.

Higgins, J. and Schrag, D. (2012) Records of Neogene seawater chemistry and diagenesis in deep-sea carbonate sediments and pore fluids. Earth and Planetary Science Letters 357, 386-396.

Horita, J., Zimmermann, H. and Holland, H.D. (2002) Chemical evolution of seawater during the Phanerozoic. Geochimica et Cosmochimica Acta 66, 3733-3756.

Hover, V.C., Walter, L.M. and Peacor, D.R. (2001) Early marine diagenesis of biogenic aragonite and Mg-calcite: new constraints from high-resolution STEM and AEM analyses of modern platform carbonates. Chemical Geology 175, 221-248.

Ingram, B. and Sloan, D. (1992) Strontium isotopic composition of estuarine sediments as paleosalinity-paleoclimate indicator. Science 255, 68.

Katz, A. (1973) The interaction of magnesium with calcite during crystal growth at 25–90°C and one atmosphere. Geochimica et Cosmochimica Acta 37, 1563-1586.

Khalifa, G.M., Kirchenbuechler, D., Koifman, N., Kleinerman, O., Talmon, Y., Elbaum, M., Addadi, L., Weiner, S. and Erez, J. (2016) Biomineralization pathways in a foraminifer revealed using a novel correlative cryo-fluorescence–SEM–EDS technique. Journal of Structural Biology 196, 155-163.

Kozdon, R., Kelly, D., Kitajima, K., Strickland, A., Fournelle, J. and Valley, J. (2013) In situ δ18O and Mg/Ca analyses of diagenetic and planktic foraminiferal calcite preserved in a deep-sea record of the Paleocene-Eocene thermal maximum. Paleoceanography 28, 517-528.

Kroenke, L.W., Berger, W.H. and Janecek, T.R. (1991) Site 807. Proceedings of the Ocean Drilling Program, Initial Reports 130, 369-493.

Land, L.S. (1967) Diagenesis of skeletal carbonates. Journal of Sedimentary Research 37.

Lea, D.W., Martin, P.A. and Spero, H. (1995) Calcium uptake and calcification rate in the planktonic foraminifer Orbulina universa. Oceanographic Literature Review 10, 865-866.

Lea, D.W., Mashiotta, T.A. and Spero, H.J. (1999) Controls on magnesium and strontium uptake in planktonic foraminifera determined by live culturing. Geochimica et Cosmochimica Acta 63, 2369-2379.

Lea, D.W., Pak, D.K. and Spero, H.J. (2000) Climate impact of late Quaternary equatorial Pacific sea surface temperature variations. Science 289, 1719-1724.

Lear, C., Elderfield, H. and Wilson, P. (2000) Cenozoic deep-sea temperatures and global ice volumes from Mg/Ca in benthic foraminiferal calcite. Science 287, 269-272.

Lear, C.H., Rosenthal, Y. and Slowey, N. (2002) Benthic foraminiferal Mg/Ca-paleothermometry: A revised core-top calibration. Geochimica et Cosmochimica Acta 66, 3375-3387.

Lear, C.H., Mawbey, E.M. and Rosenthal, Y. (2010) Cenozoic benthic foraminiferal Mg/Ca and Li/Ca records: Toward unlocking temperatures and saturation states. Paleoceanography 25.

Lowenstein, T.K., Timofeeff, M.N., Brennan, S.T., Hardie, L.A. and Demicco, R.V. (2001) Oscillations in Phanerozoic seawater chemistry: Evidence from fluid inclusions. Science 294, 1086-1088.

Mavromatis, V., Gautier, Q., Bosc, O. and Schott, J. (2013) Kinetics of Mg partition and Mg stable isotope fractionation during its incorporation in calcite. Geochimica et Cosmochimica Acta 114, 188-203.

Millero, F.J. (1982) The effect of pressure on the solubility of minerals in water and seawater. Geochimica et Cosmochimica Acta 46, 11-22.

Mucci, A. (1983) The solubility of calcite and aragonite in seawater at various salinities, temperatures, and one atmosphere total pressure. American Journal of Science 283, 780-799.

Mucci, A. and Morse, J.W. (1983) The incorporation of Mg2+ and Sr2+ into calcite overgrowths: influences of growth rate and solution composition. Geochimica et Cosmochimica Acta 47, 217-233.

Mucci, A. and Morse, J.W. (1984) The solubility of calcite in seawater solutions of various magnesium concentration, It= 0.697 m at 25 C and one atmosphere total pressure. Geochimica et Cosmochimica Acta 48, 815-822.

Mucci, A. (1987) Influence of temperature on the composition of magnesian calcite overgrowths precipitated from seawater. Geochimica et Cosmochimica Acta 51, 1977-1984.

Navrotsky, A. and Capobianco, C. (1987) Enthalpies of formation of dolomite and of magnesian calcites. American Mineralogist 72, 782-787.

Nielsen, L.C., De Yoreo, J.J. and DePaolo, D.J. (2013) General model for calcite growth kinetics in the presence of impurity ions. Geochimica et Cosmochimica Acta 115, 100-114.

Nordstrom, D.K. and Munoz, J.L. (1986) Geochemical Thermodynamics. Blackwell Scientific Publications, Palo Alto, California.

Nürnberg, D., Bijma, J. and Hemleben, C. (1996) Assessing the reliability of magnesium in foraminiferal calcite as a proxy for water mass temperatures. Geochimica et Cosmochimica Acta 60, 803-814.

Oomori, T., Kaneshima, H., Maezato, Y. and Kitano, Y. (1987) Distribution coefficient of Mg2+ ions between calcite and solution at 10–50 C. Marine Chemistry 20, 327-336.

Paquette, J. and Reeder, R.J. (1995) Relationship between surface structure, growth mechanism, and trace element incorporation in calcite. Geochimica et Cosmochimica Acta 59, 735-749.

Plummer, L.N. and Mackenzie, F.T. (1974) Predicting mineral solubility from rate data; application to the dissolution of magnesian calcites. American Journal of Science 274, 61-83.

Plummer, L.N. and Busenberg, E. (1982) The solubilities of calcite, aragonite and vaterite in CO2-H2O solutions between 0 and 90 C, and an evaluation of the aqueous model for the system CaCO3-CO2-H2O. Geochimica et Cosmochimica Acta 46, 1011-1040.

Raitzsch, M., Dueñas-Bohórquez, A., Reichart, G.-J., de Nooijer, L.J. and Bickert, T. (2010) Incorporation of Mg and Sr in calcite of cultured benthic foraminifera: impact of calcium concentration and associated calcite saturation state. Biogeosciences 7, 869-881.

Reeder, R.J. (2000) Constraints on cation order in calcium-rich sedimentary dolomite. Aquatic Geochemistry 6, 213-226.

Richter, F.M. and DePaolo, D.J. (1987) Numerical models for diagenesis and the Neogene Sr isotopic evolution of seawater from DSDP Site 590B. Earth and Planetary Science Letters 83, 27-38.

Richter, F.M. and Liang, Y. (1993) The rate and consequences of Sr diagenesis in deep-sea carbonates. Earth and Planetary Science Letters 117, 553-565.

Rosenthal, Y., Boyle, E.A. and Slowey, N. (1997) Temperature control on the incorporation of magnesium, strontium, fluorine, and cadmium into benthic foraminiferal shells from Little Bahama Bank: Prospects for thermocline paleoceanography. Geochimica et Cosmochimica Acta 61, 3633-3643.

Schiebel, R. (2002) Planktic foraminiferal sedimentation and the marine calcite budget. Global Biogeochemical Cycles 16.

Schrag, D.P., Higgins, J.A., Macdonald, F.A. and Johnston, D.T. (2013) Authigenic carbonate and the history of the global carbon cycle. Science 339, 540-543.

Segev, E. and Erez, J. (2006) Effect of Mg/Ca ratio in seawater on shell composition in shallow benthic foraminifera. Geochemistry, Geophysics, Geosystems 7.

Shackleton, N. (1987) Oxygen isotopes, ice volume and sea level. Quaternary Science Reviews 6, 183-190.

Toyofuku, T., Kitazato, H., Kawahata, H., Tsuchiya, M. and Nohara, M. (2000) Evaluation of Mg/Ca thermometry in foraminifera: Comparison of experimental results and measurements in nature. Paleoceanography 15, 456-464.

Tyrrell, T. and Zeebe, R.E. (2004) History of carbonate ion concentration over the last 100 million years. Geochimica et Cosmochimica Acta 68, 3521-3530.

Vinograd, V.L., Winkler, B., Putnis, A., Gale, J.D. and Sluiter, M.H. (2006) Static lattice energy calculations of mixing and ordering enthalpy in binary carbonate solid solutions. Chemical Geology 225, 304-313.

Walter, L.M. (1984) Magnesian calcite stabilities: A reevaluation. Geochimica et Cosmochimica Acta 48, 1059-1069.

Winland, H.D. (1969) Stability of calcium carbonate polymorphs in warm, shallow seawater. Journal of Sedimentary Research 39.

Zachos, J.C., Stott, L.D. and Lohmann, K.C. (1994) Evolution of early Cenozoic marine temperatures. Paleoceanography 9, 353-387.

AUTHOR CONTRIBUTIONS. L.N.L. proposed the project based on previous work. E.H.M. performed the electron microprobe work and image post-processing and assisted with manuscript preparation and revisions, and L.N.L. performed thermodynamic modeling and wrote the manuscript.

AUTHOR INFORMATION. The authors declare no competing financial interests. Correspondence and requests for materials should be addressed to lnlammers@berkeley.edu.